Blocking the apolipoprotein E/amyloid-β interaction as a potential therapeutic approach for Alzheimer's disease

Martin J. Sadowski*†‡, Joanna Pankiewicz*, Henrieta Scholtzova*, Pankaj D. Mehta§, Frances Prelli*, David Quartermain*, and Thomas Wisniewski*†§¶

Departments of *Neurology, †Psychiatry, and ¶Pathology, New York University School of Medicine, 550 First Avenue, New York, NY 10016; and §New York State Institute for Basic Research in Developmental Disabilities, 1050 Forest Hill Road, Staten Island, NY 10314

The amyloid-β (Aβ) cascade hypothesis of Alzheimer's disease (AD) maintains that accumulation of Aβ peptide constitutes a critical event in the early disease pathogenesis. The direct binding between Aβ and apolipoprotein E (apoE) is an important factor implicated in both Aβ clearance and its deposition in the brain's parenchyma and the walls of meningoencephalic vessels as cerebral amyloid angiopathy. With the aim of testing the effect of blocking the apoE/Aβ interaction in vivo as a potential novel therapeutic target for AD pharmacotherapy, we have developed Aβ12-28P, which is a blood-brain-barrier-permeable nontoxic, and nonfibrillogenic synthetic peptide homologous to the apoE binding site on the full-length Aβ. Aβ12-28P binds with high affinity to apoE, preventing its binding to Aβ, but has no direct effect on Aβ aggregation. Aβ12-28P shows a strong pharmacological effect in vivo. Its systemic administration resulted in a significant reduction of Aβ plaques and cerebral amyloid angiopathy burden and a reduction of the total brain level of Aβ in two AD transgenic mice models. The treatment did not affect the levels of soluble Aβ fraction or Aβ oligomers, indicating that inhibition of the apoE/Aβ interaction in vivo has a net effect of increasing Aβ clearance over deposition and at the same time does not create conditions favoring formation of toxic oligomers. Furthermore, behavioral studies demonstrated that treatment with Aβ12-28P prevents a memory deficit in transgenic animals. These findings provide evidence of another therapeutic approach for AD.

Alzheimer's pathology | memory loss prevention | peptide | transgenic mice | treatment

Alzheimer's disease (AD) is the most common neurodegenerative disease worldwide, characterized by a progressive dysfunction in multiple cognitive domains and complex neuropathological features that include accumulation of amyloid-β (Aβ) followed by synaptic dysfunction, formation of neurofibrillary tangles, and neuronal loss. With the expected increase in AD prevalence, as a function of the population aging, effective treatment for AD is critically needed. Multiple lines of evidence indicate that a disturbance of Aβ homeostasis is a paramount event in early disease pathogenesis (1). Aβ is a hydrophobic 39- to 43-aa peptide, which is derived from cleavage of a larger, synaptic transmembrane protein, the amyloid precursor protein (APP) (2). The accumulation of Aβ in the brain is determined by the rate of its generation versus in situ proteolytic degradation and clearance across the blood-brain-barrier [BBB; for review see Tanzi et al. (3)]. In the setting of increased concentration, Aβ monomers assemble into oligomers and fibrils and eventually become deposited, forming parenchymal plaques and cerebral amyloid angiopathy (CAA).

Inheritance of the apolipoprotein E4 (apoE4) allele is the strongest genetic risk factor identified so far. ApoE isotype inheritance modulates the prevalence, age of onset, and the burden of pathology in sporadic AD (4, 5). ApoE binds Aβ with high affinity and acts as a "double-edged sword" in the pathomechanism of AD, being involved in both clearance of Aβ across

the BBB (6, 7) and the promotion of its deposition (5, 8, 9). All human apoE isoforms (E2, E3, and E4) promote in vivo assembly of Aβ synthetic peptide into fibrils and enhance Aβ toxicity in tissue culture with E4 producing the most striking effect (10–12). Knockout of the apoE gene (apoE$_{KO}$) in APP$_{V717F}$ AD transgenic (Tg) mice results in a dramatic reduction in Aβ burden associated with a virtual absence of parenchymal fibrillar Aβ deposits and CAA (13–15). These observations indicate that the net effect of apoE's involvement in Aβ metabolism favors its deposition over the clearance and also suggests that pharmacological blockade or neutralization of the apoE/Aβ interaction may provide an alternative therapeutic strategy. We and others have demonstrated that short synthetic peptides corresponding to Aβ residues 12–28, which is the apoE binding motif on Aβ, can bind to lipidated human apoE and abolish its effect on Aβ aggregation and toxicity in cell culture (12, 16). With the aim of testing the effect of blocking the apoE/Aβ interaction on AD pathology in AD Tg models, we have designed a compound based on the Aβ12-28 sequence that was modified for in vivo administration. In the compound, Aβ12-28P, the valine in position 18 was exchanged for proline, rendering it nontoxic and nonfibrillogenic, and thus preventing the possibility of codeposition on existing plaques. Aβ12-28P was synthesized by using D-amino acids and end-protected by acetylation and amidation of the N and C termini, respectively. These modifications decreased the potential immunogenicity and extended the serum half-live (62 ± 7 min; mean ± SEM) but did not affect the ability of Aβ12-28P to inhibit apoE/Aβ binding (12, ‖, **). Aβ12-28P is BBB-permeable as has been demonstrated (12). Here, we present results of in vivo studies in two different AD Tg models where Aβ12-28P was used to block the apoE/Aβ interaction. Our results indicate that compounds antagonizing the apoE/Aβ interaction constitute an effective therapeutic approach for AD.
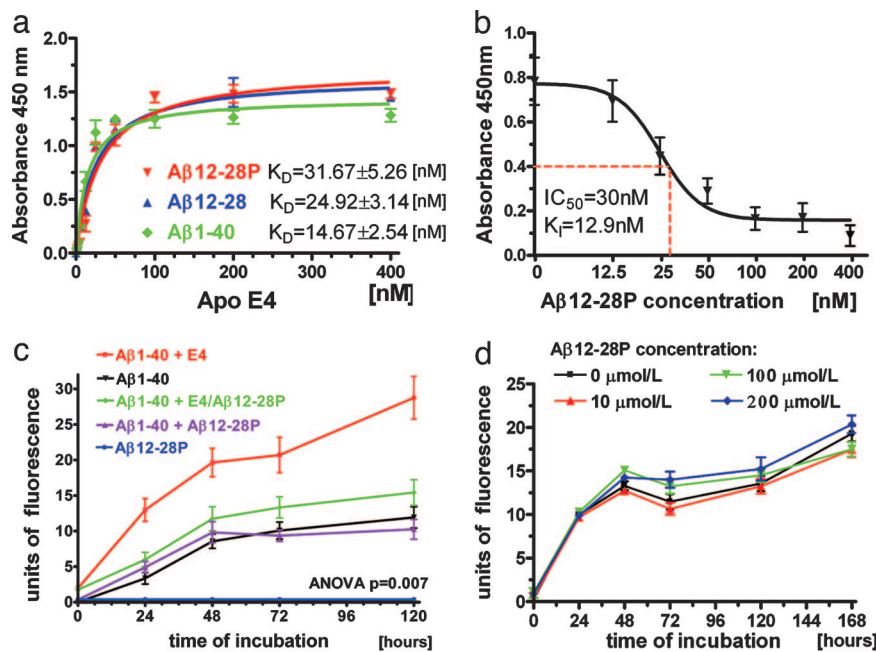
NEUROSCIENCE

Fig. 1. Aβ12-28P binds to apoE and abolishes its effect on Aβ fibrillization. (*a*) Shown is a solid-phase binding assay of lipidated human apoE4 isoform to Aβ1-40, Aβ12-28P, and Aβ12-28 synthesized from L-amino acids. K_D values represent mean $\pm$ SEM from three independent experiments. (*b*) Shown is dose-dependent inhibition of the apoE4/Aβ binding by increasing concentrations of Aβ12-28. *P* values represent mean $\pm$ SEM from three independent experiments. (*c*) Thioflavin-T aggregation assay demonstrates the effect of Aβ12-28P on the apoE/Aβ interaction. Adding the human lipidated apoE4 complexes dramatically increases the amount of Aβ1-40 fibrils formed over time ($P = 0.007$, repeated measures ANOVA; $P < 0.01$ for specific post hoc comparison of Aβ1-40 + apoE4 versus Aβ1-40 alone). Preincubation of apoE with Aβ12-28P abolishes the apoE effect on Aβ1-40 aggregation ($P < 0.01$ and nonsignificant post hoc analysis for the specific effect of Aβ+apoE/Aβ12-28P versus Aβ + apoE and Aβ, respectively). Aβ12-28P alone has no effect on the aggregation of Aβ1-40 (nonsignificant). Aβ12-28P does not aggregate over time. (*d*) Shown is a lack of direct effect of Aβ12-28P on Aβ1-40 aggregation. Aβ1-40 (200 μmol/liter) was incubated in the presence of Aβ12-28P concentrations ranging from 0 to 200 μmol/liter (repeated measures ANOVA $P = 0.573$).

Results and Discussion

Effect of Aβ12-28P on the ApoE/Aβ Interaction and Aβ1-40 Aggregation *in Vitro*. The dissociation constant (K_D) between Aβ12-28P and lipidated human apoE4 isoform was determined to be 31.67 ± 5.26 nM, which was comparable to that of Aβ12-28 synthesized with L-amino acids without any terminal modifications, and only twice as high as the K_D of the binding between lipidated apoE4 and Aβ1-40 (Fig. 1*a*). In a competitive inhibition assay Aβ12-28P was demonstrated to inhibit the binding of lipidated apoE4 to Aβ1-40 in a concentration-dependent manner. Half-maximal inhibition (IC$_{50}$) derived from a one-site competition, nonlinear regression equation was 30 nM, whereas the inhibition constant (K_I) was calculated based on the previously determined K_D to be 12.9 nM (Fig. 1*b*). The ability of Aβ12-28P to neutralize apoE's promoting effect on Aβ1-40 fibrillization was demonstrated by using an *in vitro* aggregation assay. Whereas adding the lipidated apoE4 isoform dramatically increased amount of Aβ1-40 fibrils formed over time, this effect was abolished by preincubation of apoE4 with Aβ12-28P. Aβ12-28P showed no direct effect on Aβ1-40 fibrillization even at a concentration of 200 μmol/liter (Fig. 1 *c* and *d*). Results of these *in vitro* experiments indicate that the effect of Aβ12-28P on Aβ fibrillization is exerted only through blocking the apoE/Aβ interaction, with Aβ12-28P having no direct effect on Aβ aggregation.

Treatment of Tg Mice with Aβ12-28P: Monitoring the Immune Response and Serum Lipid Level. We administered Aβ12-28P or vehicle to Tg mice carrying a Swedish K670L/M671L APP mutation (APP$_{SWE}$) from the age of 12 to 18 months and to double Tg mice carrying an additional presenilin 1 M146L mutation (APP$_{SWE}$/PS1) from the age of 2 to 7 months. The treatment was initiated at the time when the first brain Aβ deposits appear in those models. During the treatment animals were closely monitored for signs of toxicity, and

after death their organs were examined for any signs of pathology. We did not notice any symptoms indicating altered behavior, signs of systemic toxicity, organ damage, or, in particular, systemic amyloidosis.

An immune response against Aβ was closely monitored to assure that the treatment effect was not associated with a vaccination effect. There were no anti-Aβ antibodies present in the pretreatment and posttreatment sera of APP$_{SWE}$/PS1 mice and pretreatment sera of APP$_{SWE}$ mice. The anti-Aβ antibodies were detected in the posttreatment sera of 18-month-old APP$_{SWE}$ mice, which received either vehicle or Aβ12-28P. Their levels was estimated at 1.7 ± 0.5 μg (mean $\pm$ SEM) and 1.9 ± 0.3 μg for IgM class, and 2.6 ± 0.4 μg and 3.2 ± 0.7 for IgG class in vehicle- and Aβ12-28P-treated groups, respectively. Differences between groups were not statistically significant.

Because a compound targeting apoE could hypothetically affect the serum lipid level, the total cholesterol level and apoE level were monitored during treatment. The total serum cholesterol level was higher by 12.3% in APP$_{SWE}$ mice and 8.4% in APP$_{SWE}$/PS1 mice in groups treated with Aβ12-28P [difference is nonsignificant; supporting information (SI) Fig. 6 *a* and *b*]. The serum apoE level showed no differences by Western blot. Because the posttreatment sera were collected 1 week after the last dose of Aβ12-28P (at the time when animals were killed) we performed an additional experiment where the total cholesterol level in the serum was followed by repetitive measurement after a single i.v. administration of Aβ12-28P. In this experiment, a transient increase in the total cholesterol level was observed, which had a peak at 72 h after injection (147.6% of the baseline total cholesterol value $P < 0.001$; SI Fig. 7) and returned back to baseline within the next 4 days. This finding indicates that the biological activity of Aβ12-28P involves an effect on the serum lipid profile that is transient and reversible.
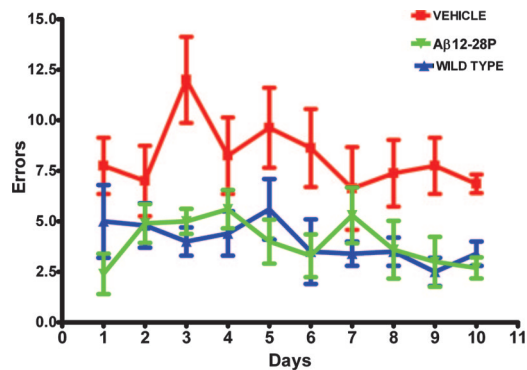
Fig. 2. Treatment with Aβ12-28P rescues APP$_{K670N/M671L}$ mice from memory decline. Aβ12-28P-treated APP$_{K670N/M671L}$ mice performed comparably to WT, age- and sex-matched littermates on radial arm maze testing. Both groups performed statistically better than APP$_{K670N/M671L}$ mice treated with vehicle; ANOVA $P < 0.0001$, post hoc Aβ12-28P vs. WT nonsignificant, Aβ12-28P vs. vehicle $P < 0.001$, WT vs. vehicle $P < 0.001$ ($n = 11$ for vehicle and Aβ12-28P-treated Tg groups, $n = 12$ for WT).

Behavioral Studies. APP$_{SWE}$ mice were subjected to behavioral testing with the radial arm maze, which assesses the working memory based on an animal's exploratory behavior (19). The testing was performed during the last month of the experiment (between ages 17 and 18 months) while animals were still receiving Aβ12-28P or vehicle. The performance of APP$_{SWE}$ mice was compared with that of age- and sex-matched WT littermates. The treatment with Aβ12-28P prevented memory deficit in APP$_{SWE}$ mice. Aβ12-28P-treated APP$_{SWE}$ and WT mice performed comparably (Fig. 2; no statistically significant difference), whereas both groups were significantly better than the vehicle-treated APP$_{SWE}$ mice (ANOVA $P < 0.0001$, post hoc $P < 0.001$ for each pair of groups).

Quantification of Aβ Deposition. The burden of Aβ plaques (the percentage of test area occupied by parenchymal Aβ deposits, excluding Aβ-laden vessels) was examined by using a semiautomated image analyzing system and unbiased, hierarchical random sampling scheme by an investigator blinded to the animal treatment status (J.P.). The Aβ burden was evaluated separately on the immunostained section (total Aβ burden) and in sections stained with Thioflavin-S (fibrilar Aβ burden) in the neocortex, cingulate cortex, and hippocampus. Anti-Aβ immunohistochemistry was performed by using a mixture of mAbs 6E10 (recognizing Aβ residues 1–16) and 4G8 (recognizing Aβ residues 17–24) (9). A mixture of mAbs was used to increase the signal intensity, reduce background, and avoid the possibility that Aβ12-28P could interact with existing deposits and mask the 4G8 epitope. The total Aβ burden in the neocortex of Aβ12-28P-treated APP$_{SWE}$ mice was lower by 51.6% compared with the vehicle-treated group ($P < 0.001$), whereas in the cingulated cortex and hippocampus it was lower by 53.4% and 45.6% ($P < 0.01$), respectively (Fig. 3a). A comparably degree of reduction was noted in APP$_{SWE}$/PS1 double Tg animals: 50.7% in the neocortex, 49.2% in the cingulate cortex, and 40.0% in the hippocampus ($P < 0.01$; Fig. 3 a and b).

Staining with Thioflavine-S reveals only the fibrillar component of Aβ deposits. They constitute a fraction of the Aβ burden in the parenchyma and the entire CAA burden. Fibrillar Aβ deposits in both the parenchyma and the vessels are known to contain codeposited fragments of apoE (9). In addition, the parenchymal fibrillar deposits are associated with neuritic degeneration (14). The treatment of APP$_{SWE}$ mice with Aβ12-28P resulted in a reduction of the fibrillar Aβ burden in the neocortex, cingulate cortex, and hippocampus by 38.0%, 38.7%, and 31.9% ($P < 0.05$), respectively (Fig. 3 c and d). In APP$_{SWE}$/PS1
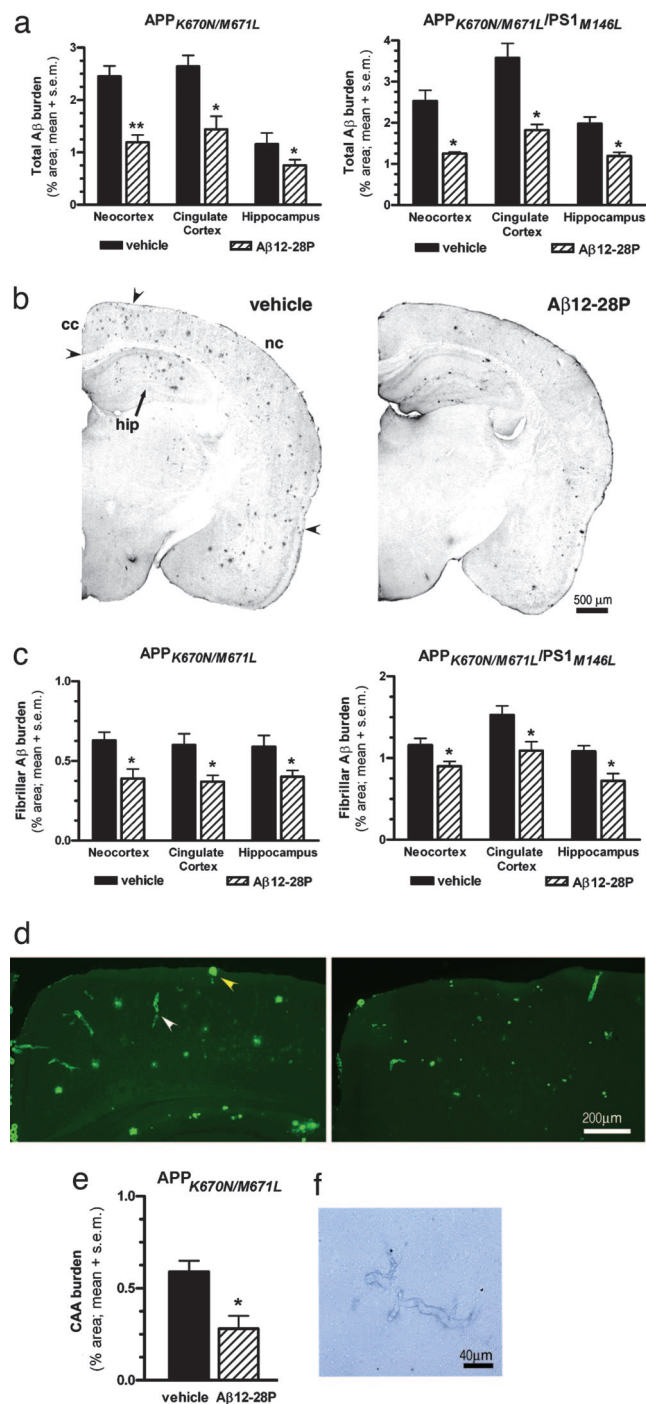

Fig. 3. Treatment with Aβ12-28P reduces Aβ deposition in APP$_{K670N/M671L}$ and APP$_{K670N/M671L}$/PS1$_{M146L}$ mice. (*a*) Decrease in the total Aβ burden in the neocortex, the cingulated cortex, and the hippocampus as quantified by unbiased hierarchical sampling ($n = 11$; *, $P < 0.01$; **, $P < 0.001$). (*b*) Hemispheric sections from 7-month-old APP$_{K670N/M671L}$/PS1$_{M146L}$ mice treated with vehicle (*Left*) and Aβ12-28P (*Right*) depict the difference in Aβ burden. Immunostaining was done with a mixture of 4G8 and 6E10 anti-Aβ mAbs. (*c*) Shown is a reduction in the fibrillar Aβ burden in Aβ12-28P-treated animals ($n = 11$; *, $P < 0.05$). (*d*) Shown is the cingulate cortex and the neocortex of 18-month-old vehicle-treated (*Left*) and Aβ12-28P-treated (*Right*) APP$_{K670N/M671L}$ mice stained with Thioflavin-S. There is a clearly visible reduction in the burden of parenchymal Aβ deposits (yellow arrowhead) and CAA (white arrowhead). Both types of deposits were quantified separately. (*e*) Shown is a decrease in the CAA burden in Aβ12-28P-treated APP$_{K670N/M671L}$ mice (*, $P < 0.05$). (*f*) Shown is Perls staining of parenchymal vessels in Aβ12-28P-treated APP$_{K670N/M671L}$ mice, revealing a lack of microhemorrhages.
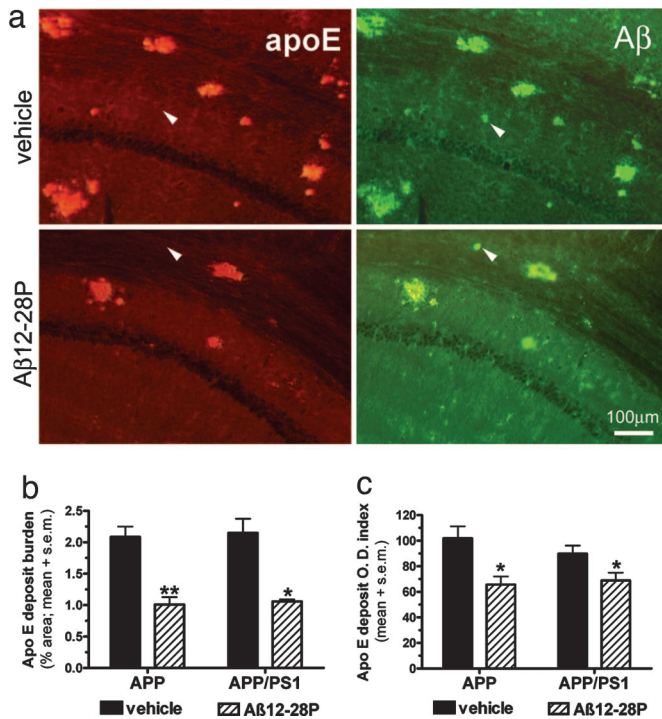
NEUROSCIENCE

Fig. 4. Treatment with Aβ12-28P reduces the amount of apoE present in Aβ deposits. (*a*) Shown is double immunofluorescent staining colocalizating apoE in Aβ deposits in the hippocampus of APP$_{K670N/M671L}$ mice. Only a minority of plaques were apoE-negative in both groups (see white arrowheads). (*b*) Shown is a reduction in the burden of apoE-positive deposits in Aβ12-28P-treated animals (*, *P* < 0.01; **, *P* < 0.001). Values are averaged for all three areas of interest. (*c*) Shown is the reduction in the mean optic density (O.D.) index of apoE deposits in Aβ12-28P-treated animals (*, *P* < 0.05).
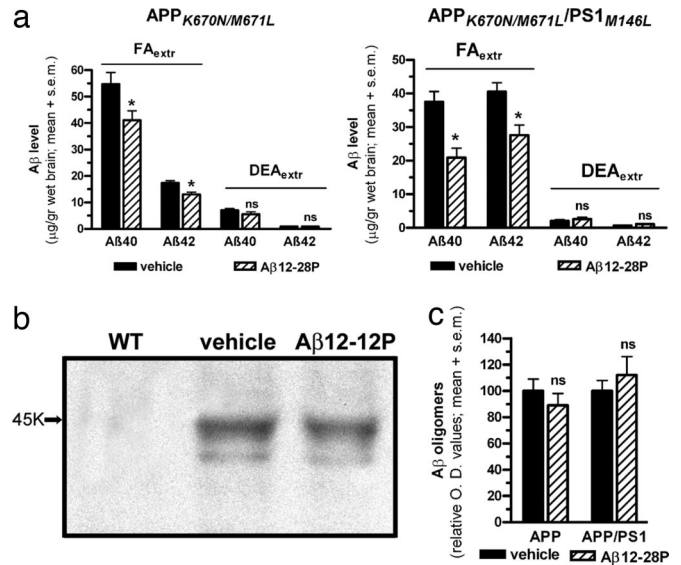

Fig. 5. Treatment with Aβ12-28P decreases the levels of total Aβ40 and Aβ42 but does not alter levels of the soluble Aβ fraction or Aβ oligomers. (*a*) Shown is a statistically significant decrease in the levels of FA-extracted (FA$_{extr}$) Aβ40 and Aβ42 (total Aβ) in APP$_{K670N/M671L}$ mice (*Left*) and APP$_{K670N/M671L}$/PS1$_{M146L}$ mice (*Right*). The level of soluble Aβ40 and Aβ42 fractions extracted with DEA (DEA$_{extr}$) did not differ between groups (*n* = 11; *, *P* < 0.05; ns, not significant). (*b*) A Western blot of brain homogenates stained with A11 oligomer-specific polyclonal antibody. The density and thickness of oligomer bands did not differ between vehicle-and Aβ12-28P-treated 18-month-old APP$_{K670N/M671L}$ mice. No oligomers were detected in age-matched WT littermates. (*c*) The densitometric analysis of oligomer-specific bands. There is no significant difference between Aβ12-28P- and vehicle-treated groups in either Tg model.

mice the treatment produced a 21.9%, 28.9%, and 32.7% reduction (*P* < 0.05) in the respective regions.

In addition to the analysis of the Aβ burden in the parenchyma, we evaluated the treatment effect on CAA in APP$_{SWE}$ mice. At the age of 18 months this model possess a substantial degree of CAA (15, 20), whereas in 7-month-old APP$_{SWE}$/PS1 the occurrence of Aβ angiopathy is still very variable, hence assessment of the treatment effect in the latter model is unreliable because of a large standard deviation among subjects. The CAA burden [i.e., a percentage of test area specifically occupied by the profiles of Aβ-laden vessels revealed by Thioflavine-S staining (15, 20)] was quantified by using the same principle of a hierarchical unbiased sampling scheme. A 68.4% (*P* < 0.01) reduction in the CAA burden of the penetrating cortical vessels (analyzed together in the cingulate cortex and neocortex) was noted in the Aβ12-28P-treated animals (Fig. 3 *d* and *e*). The integrity of cerebral vessels was examined in Aβ12-28P- and vehicle-treated APP$_{SWE}$ mice on sections stained with hematoxilin and eosin using the Perls method that detects hemosiderin, indicating previous hemorrhage (15, 21). We did not detect evidence of micro or macro hemorrhages in association with Aβ12-28P treatment in brains of 18-month-old APP$_{SWE}$ mice (Fig. 3*f*).

Quantification of ApoE Deposition Within Aβ Plaques. ApoE-positive deposits were evaluated on a separate set of sections by using double immunofluorescent staining for Aβ and apoE (Fig. 4*a*). The burden of apoE-positive deposits was quantified in an analogous manner to that used to measure the Aβ burden. The burden of apoE deposits was reduced by 51.9% in APP$_{SWE}$ mice (*P* < 0.001) and 50.9% in APP$_{SWE}$/PS1 mice (*P* < 0.01) (Fig. 4 *a* and *b*). Furthermore, the mean optic density index of apoE

deposits was also reduced by 35.5% in APP$_{SWE}$ mice (*P* < 0.01) and 23% in APP$_{SWE}$/PS1 mice (*P* < 0.05) (Fig. 4 *a* and *c*). The optic density index is defined as a sum of intensity values assigned to all pixels forming a deposit on a captured image. Results of these measurements indicate a relative reduction of apoE in the Aβ deposits of Aβ12-28P-treated mice.

Assessment of Aβ Level in the Brain. A potential concern related to approaches targeting Aβ is that the level of soluble Aβ could increase, producing conditions that favor formation of toxic Aβ-derived diffusible ligands (ADDLs), also known as Aβ oligomers (22). This situation could paradoxically potentiate Aβ neurotoxicity and exacerbate cognitive deficit, especially in the situation when Aβ clearance could be impaired. ELISA measurements of Aβ level in the formic acid (FA)-extracted samples of brain homogenate revealed reductions of Aβ40 and Aβ42 species in Aβ12-28P-treated APP$_{SWE}$ mice by 24.7% and 25.0% (*P* < 0.05), respectively. In APP$_{SWE}$/PS1 mice the reductions were 44.3% and 31.6% (*P* < 0.05), respectively (Fig. 5*a*). The measure of the soluble Aβ fraction, which is considered to contain ADDLs, was performed in the separate, diethylamine (DEA)-extracted samples. There were no statistically significant differences between Tg animals that received Aβ12-28P or vehicle. DEA-released fractions of Aβ species constituted from 1.7% to 13.6% of those FA extracted (Fig. 5*a*). In addition, the level of Aβ oligomers in the brain homogenate was assessed by nonreducing, SDS/PAGE using the A11 oligomer-specific antibody (23, 24). No differences were found between Aβ12-28P- and vehicle-treated Tg mice, and no oligomers were detected in WT animals (Fig. 5 *b* and *c*).

Discussion

The apoE/Aβ interaction plays an important role in the conformational transformation of soluble Aβ and the formation of Aβ

deposits in the AD brain. Here we have *in vivo*-analyzed the effect of blocking the apoE/Aβ interaction as a potential therapeutic approach for AD. We have used Aβ12-28P, which is a nonimmunogenic, BBB-permeable, short synthetic peptide with an extended serum half-life [see results of previous studies on the development and *in vitro* characteristic of Aβ12-28P (12)]. Aβ12-28P binds to apoE and prevents its binding to full-length Aβ, which abolishes apoE's effect on Aβ fibril formation. Aβ12-28P has no direct effect on Aβ aggregation. In the current studies we have demonstrated that Aβ12-28P is also effective *in vivo*, reducing both the burden of Aβ deposits and the total Aβ level in the brains of two AD Tg model mice. Because of its D-amino acid composition, Aβ12-28P does not cause an immune response; therefore, its therapeutic effect cannot be explained by a vaccination phenomenon. In addition to reducing Aβ parenchymal deposits, treatment with Aβ12-28P resulted in a significant reduction in the CAA burden, which was not associated with any perivascular hemorrhages. This observation demonstrates an additional therapeutic benefit of blocking the apoE/Aβ interaction that has not been observed with immunization against Aβ. Anti-Aβ immunization approaches do not effectively reduce the CAA burden and, in addition, may increase the risk of cerebral hemorrhages because of an immune process taking place in the weakened vascular wall (21).

A hypothetical risk associated with approaches targeting Aβ aggregation and deposition involves increasing the pool of soluble Aβ, which in turn may create conditions favoring formation of toxic oligomers. This concern is especially pertinent in the case of Aβ12-28P as apoE has been considered to play an important role in the clearance of Aβ across the BBB. We have demonstrated that although treatment with Aβ12-28P results in a decrease in parenchymal and vascular Aβ deposits along with a decrease in the total Aβ level, the level of soluble Aβ and the level of oligomers remain stable. This finding suggests that any excess of soluble Aβ not aggregated in plaques is either destroyed *in situ* by Aβ degrading enzymes or is transported out from the brain by nonapoE-dependent mechanisms. Although early studies implicated apoE in Aβ's clearance as one of the lipoprotein receptor-related protein 1 (LRP) ligands (7), more recent studies have shown that this process is not exclusively apoE-dependent as several other Aβ binding proteins may serve as LRP ligands (25). Furthermore, recent evidence indicates that Aβ may binds to LRP directly, a process that is responsible for the major of Aβ efflux at brain capillaries (26). Also apoE knockout in AD Tg mice demonstrated that the net effect of the apoE/Aβ interaction favors Aβ deposition over its clearance (13).

Although, the half-life of Aβ12-28P is relatively short (62.7 min) its therapeutic effect appears to be prolonged. This phenomenon may be explained by the high binding affinity Aβ12-28P has for apoE, which results in the neutralization of apoE's ability to chaperone the assembly of Aβ into fibrils. A return of apoE's fibril promotion requires generation of new apoE molecules. Similarly a prolonged biological effect of Aβ12-28P on total serum cholesterol level can be demonstrated, which is maintained for several days after a single injection (see SI Fig. 7).

Unlike mice, human apoE exists in three isoforms (E2, E3, and E4) with single amino acid differences at positions 112 and 158, which have significantly different effects on Aβ deposition (5). Studies using Tg models expressing human apoE3 or apoE4 isoforms demonstrated that compared with apoE$_{KO}$ mice human apoE enhances Aβ deposition, with E4 producing the strongest effect (14, 20). Therefore, agents blocking the apoE/Aβ interaction could be applied to human subjects with various apoE backgrounds, with the expectation of the greatest impact in E4 homozygotes.

Aβ12-28P can be considered a lead compound in further development of pharmaceuticals, antagonizing the apoE/Aβ interaction suitable for clinical application. Resistance to destruction in the alimentary tract and improved pharmacokinetic parameters could be achieved by using peptidomimetic technology. Peptoids, because

of their inherent biomimetic character, broad chemical diversity, and facile synthesis, are an attractive platform for the discovery of novel therapeutic compounds that are potentially feasible for clinical application. A point to consider in future drug design is that we have demonstrated that Aβ12-28P has the potential to raise serum cholesterol. Therefore the effect of future compounds on serum cholesterol levels has to be closely monitored. Fortunately, the elevation of cholesterol level appears to be reversible.

A critical need exists for more effective forms of therapy for AD, because of its high prevalence, which is expected to increase even further in the coming decades with the aging of society. Compounds blocking the apoE/Aβ interaction constitute an additional therapeutic approach that targets an alternative pathway contributing to disease progress. This approach does not preclude the combined use of other emerging treatment strategies such as secretase inhibitors or passive immunization, which may have a synergistic effect to enhance the overall therapeutic outcome.

Materials and Methods

Unless stated otherwise all reagents and antibodies were purchased from Sigma-Aldrich (St. Louis, MO). Aβ1-40, Aβ12-28, and Aβ12-28P peptides were custom-synthesized at the W. M. Keck Facility at Yale University (New Haven, CT) by using solid-phase support, and they were purified as described (11, 12, 19). Aβ12-28P used for *in vitro* assays was derived from the same batch administered to Tg animals. Lipidated apoE4 complexes were prepared from primary astrocytic cultures derived from apoE4 Tg mice as described (12). Anti-Aβ antibodies were provided by P.D.M.

ApoE/Aβ12-28P Binding Studies, Competitive Inhibition, and Aggregation Assays. The dissociation constant (K_D) between lipidated human apoE4 and Aβ12-28P, Aβ12-28 (L-amino acid), and Aβ1-40 were determined from a one-site binding nonlinear regression equation. The competitive inhibition assay of apoE/Aβ1-40 binding by Aβ12-28P was performed as described (12). Values of half-maximal inhibition (IC_{50}) and the inhibition constant (K_I) were derived from a one-site competition, nonlinear regression equation calculated by using Prism 4.01 (GraphPad Software Inc., San Diego, Ca).

In aggregation experiment samples containing Aβ1-40 (100 μmol/liter) and Aβ1-40 together with apoE (2 μmol/liter) and/or Aβ12-28P (4 μmol/liter) were incubated in 0.1 mol/liter of Tris buffer (pH 7.0) at 37°C. Before the aggregation studies Aβ1-40 was treated with 1,1,1,3,3,3-hexafluoro-2-propanol to assure complete disaggregation and monomerization (12). The amount of Aβ1-40 fibrils formed over time was determined by a standard Thioflavin-T assay performed according to previously published protocols (11, 12, 19).

AD Tg Mice. Studies were performed on female APP$_{K670L/M671L}$ and APP$_{K670L/M671L}$/PS1$_{M146L}$ Tg mice. Non-Tg, female littermates were used as age-matched control for behavioral testing and for lipid studies (see SI *Materials and Methods* for details on animals husbandry and genotyping). Animals received 1 mg of Aβ12-28P diluted under sterile condition in 0.5 ml of normal saline or the saline alone (vehicle) three times per week. The compound was administered via i.p. injection with a 27-gauge needle. Veterinary staff monitored animals weekly for any signs of toxicity or adverse reaction to the treatment, including changes in body weight, physical appearance, measurable clinical signs, unprovoked behavior, and response to external stimuli. All mouse care and experimental procedures were approved by the Institutional Animal Care and Use Committee of New York University School of Medicine. Animals were killed a week after administration of the last dose of Aβ12-28P. At the time of death samples of the heart, lungs, liver, kidney, spleen, and skeletal muscles were collected, fixed, embedded in paraffin, and stained with hematoxilin/eosin and Congo red

for detection of systemic amyloidosis. Examination was performed by T.W. who is a board-certified pathologist.

ELISA for Anti-Aβ Antibodies in the Serum. Sera collected before and after the treatment were diluted 1:200 and 1:500 and added to ELISA plates coated with synthetic Aβ1-40 50 ng per well (19). The plates were washed and incubated with specific antimouse IgG or IgM mAbs conjugated with HRP (Amersham Biosciences, Piscataway, NJ) at a 1:5,000 dilution, followed by adding 3,3,5,5-tetramethybenzidine substrate. The color reaction was stopped with 2 M sulfuric acid, and the absorbance was read at 450-nm wavelength. Sera from animals vaccinated with the peptide K6Aβ1-30 (19), which is known to induce an immune response against Aβ, and wells coated with purified murine IgG and IgM were used as positive controls, whereas sera from WT age-matched mice and uncoated wells were used as a negative controls. Each sample was tested in quadruplicate. For quantification of the antibody level a standard curve was generated by dissolving 6E10 and 4G8 antibodies (0.5 mg each) in 1 ml of WT murine serum and testing serial dilutions ranging from 1:100 to 1:3,125,000. The data were analyzed with GraphPad Prism 4.01 software. ELISA was performed by a single investigator (J.P.) blinded to animal treatment group assignment.

Radial Arm Maze Testing. The apparatus consisted of eight radial 30-cm-long arms originating from the central space. A cup baited with 0.25 ml of 0.1% saccharine solution was placed at the end of each arm. Before testing mice were deprived of water for 24 h and then their access to water was restricted to 2 h per day for the duration of testing. The task required an animal to enter all arms and drink the saccharine solution. They learned not to enter previously visited arms that were identified by specific spatial cues located around the maze. After 3 days of adaptation to the apparatus, mice were subjected to testing lasting 10 days. They were given one testing session per day during which the number of errors (entries to previously visited arms) were recorded. Behavioral testing was performed by H.S. and supervised by D.Q., both of whom were blinded to the animal's treatment status.

Unbiased Morphometric Analysis. Analysis of Aβ burden and apoE deposits was performed according to our previously published protocols using a random, unbiased, hierarchical sampling scheme on serial sections evenly spaced along the entire-rostrocaudal axis of the brain by means of a semiautomated image analysis system (9, 12, 19) (see SI *Materials and Methods* for details on tissue processing, immunostaining, and image analysis).

Sandwich ELISA for Aβ Levels. The total Aβ level and soluble Aβ fraction level extracted from the brain homogenate (see SI *Materials and Methods* for extraction details) were measured by using sandwich ELISA which uses 6E10 mAb as a capture antibody and rabbit polyclonal antibodies R162 and R165 to discriminate between the C termini of Aβ40 and Aβ42, respectively (9). The assay was performed by P.D.M., who was blinded to treatment group assignment, according to his previously published protocols (27). The levels of Aβ species in tested samples were interpolated from a standard curve prepared by serial dilution of synthetic Aβ40 and Aβ42 in comparable buffers. They were expressed as μg of Aβ per g of wet brain, taking into account the dilution during the extraction procedures ($\times 2.2$ for DEA extraction and $\times 64.15$ for FA extraction) and during brain homogenization (17).

Western Blot Detection and Quantification of Aβ Oligomers. Samples of Aβ homogenate were centrifuged at $100,000 \times g$ for 1 h (24), and the total protein concentration in the supernatant was estimated by using the bicinchoninic acid assay (BCA; Pierce, Rockford, IL). Aliquots were titrated by adding 10 mM TBS buffer (pH 7.5) to achieve a final protein concentration of 1 μg/1 μl. Ten-microliter samples, in an equal volume of sample buffer, were subjected to overnight electrophoresis on 12.5% SDS-polyacrylamide Tris-tricine gels under nonreducing conditions. Aβ oligomers were detected by using oligomer-specific A11 polyclonal antibody (Biosource, Camarillo, CA) (23). Autoradiograms were scanned and converted into eight-bit grayscale digital files. Densitometry of Aβ oligomer bands was performed with NIH Image J software, version 1.34. The specificity of A11 staining was confirmed by stripping and restaining the membranes with anti-Aβ, 6E10 antibody, which, in addition to high molecular weight bands, revealed monomeric and dimeric Aβ.

Other Measurements. Plasma lipid level was measured by a standard enzymatic assay by using a Cholesterol E kit (Wako Diagnostics, Richmond, VA) (18). The apoE serum level was estimated by SDS/PAGE of 5-μl serum samples. Western blots were developed with M-20 anti-apoE polyclonal antibody (Santa Cruz Biotechnology, Santa Cruz, CA), and densitometric analysis of autoradiograms was performed with Image J software, as described above.

Statistical Analysis. Difference between groups in Aβ burden, apoE burden, level of extracted Aβ, and level of oligomers were analyzed by using unpaired, two-tailed *t* tests. Data from the radial arm maze and Thioflavin-T aggregation assay were analyzed by repeated measures ANOVA followed by a Neuman–Keuls post hoc test, using Prism 4.01 (GraphPad, San Diego, Ca).

1. Hardy J, Selkoe DJ (2002) *Science* 297:353–356.
2. Kang J, Lemaire HG, Unterbeck A, Salbaum JM, Masters CL, Grzeschik KH, Multhaup G, Beyreuther K, Muller-Hill B (1987) *Nature* 325:733–736.
3. Tanzi RE, Moir RD, Wagner SL (2004) *Neuron* 43:605–608.
4. Mayeux R, Stern Y, Ottman R, Tatemichi TK, Tang MX, Maestre G, Ngai C, Tycko B, Ginsberg H (1993) *Ann Neurol* 34:752–754.
5. Schmechel DE, Saunders AM, Strittmatter WJ, Crain BJ, Hulette CM, Joo SH, Pericak-Vance MA, Goldgaber D, Roses AD (1993) *Proc Natl Acad Sci USA* 90:9649–9653.
6. Zlokovic BV (2004) *J Neurochem* 89:807–811.
7. Herz J (2003) *J Clin Invest* 112:1483–1485.
8. Naslund J, Thyberg J, Tjernberg LO, Wernstedt C, Karlstrom AR, Bogdanovic N, Gandy SE, Lannfelt L, Terenius L, Nordstedt C (1995) *Neuron* 15:219–228.
9. Wisniewski HM, Sadowski M, Jakubowska-Sadowska K, Tarnawski M, Wegiel J (1998) *J Neuropath Exp Neurol* 57:674–683.
10. Ma J, Yee A, Brewer HB, Jr, Das S, Potter H (1994) *Nature* 372:92–94.
11. Wisniewski T, Castaño EM, Golabek AA, Vogel T, Frangione B (1994) *Am J Pathol* 145:1030–1035.
12. Sadowski M, Pankiewicz J, Scholtzova H, Ripellino JA, Li YS, Schmidt SD, Mathews PM, Fryer JD, Holtzman DM, Sigurdsson EM, *et al.* (2004) *Am J Pathol* 165:937–948.
13. Bales KR, Verina T, Dodel RC, Du YS, Altstiel L, Bender M, Hyslop P, Johnstone EM, Little SP, Cummins DJ, *et al.* (1997) *Nat Genet* 17:263–264.
14. Holtzman DM, Bales KR, Tenkova T, Fagan AM, Parsadanian M, Sartorius LJ, Mackey B, Olney J, McKeel D, Wozniak D, *et al.* (2000) *Proc Natl Acad Sci USA* 97:2892–2897.
15. Fryer JD, Taylor JW, DeMattos RB, Bales KR, Paul SM, Parsadanian M, Holtzman DM (2003) *J Neurosci* 23:7889–7896.
16. Ma J, Brewer BH, Potter H, Brewer HB, Jr (1996) *Neurobiol Aging* 17:773–780.
17. Schmidt SD, Jiang Y, Nixon RA, Mathews PM (2005) *Methods Mol Biol* 299:267–278.
18. Trogan E, Feig JE, Dogan S, Rothblat GH, Angeli V, Tacke F, Randolph GJ, Fisher EA (2006) *Proc Natl Acad Sci USA* 103:3781–3786
19. Sigurdsson EM, Knudsen E, Asuni A, Fitzer-Attas C, Sage D, Quartermain D, Goni F, Frangione B, Wisniewski T (2004) *J Neurosci* 24:6277–6282.
20. Fryer JD, Simmons K, Parsadanian M, Bales KR, Paul SM, Sullivan PM, Holtzman DM (2005) *J Neurosci* 25:2803–2810.
21. Pfeifer M, Boncristiano S, Bondolfi L, Stalder A, Deller T, Staufenbiel M, Mathews PM, Jucker M (2002) *Science* 298:1379.
22. Walsh DM, Klyubin I, Fadeeva JV, Cullen WK, Anwyl R, Wolfe MS, Rowan MJ, Selkoe D (2002) *Nature* 416:535–539.
23. Takahashi RH, Almeida CG, Kearney PF, Yu FM, Lin MT, Milner TA, Gouras GK (2004) *J Neurosci* 24:3592–3599.
24. Gong YS, Chang L, Viola KL, Lacor PN, Lambert MP, Finch CE, Krafft GA, Klein WL (2003) *Proc Natl Acad Sci USA* 100:10417–10422.
25. Shibata M, Yamada S, Kumar S, Calero M, Bading J, Frangione B, Holtzman D, Miller CA, Strickland DK, Ghiso J, *et al.* (2000) *J Clin Invest* 106:1489–1499.
26. Deane R, Wu ZH, Sagare A, Davis J, Yan SD, Hamm K, Xu F, Parisi M, Larue B, Hu HW, *et al.* (2004) *Neuron* 43:333–344.
27. Mayeux R, Honig LS, Tang MX, Manly J, Stern Y, Schupf N, Mehta PD (2003) *Neurol* 61:1185–1190.